Larson, R. L., Lancelot, Y., et al., 1992
Proceedings of the Ocean Drilling Program, Scientific Results, Vol. 129

20. RADIOMETRIC AGES OF BASALTIC BASEMENT RECOVERED AT SITES 800, 801, AND 802, LEG 129, WESTERN PACIFIC OCEAN[1]

Malcolm S. Pringle[2]

ABSTRACT

ODP Leg 129 achieved one of its primary goals by recovering Jurassic-age ocean crust at Site 801 in the Pigafetta Basin, western Pacific Ocean. At Sites 800 and 802, although also located on presumed Jurassic-age crust, drilling terminated in the ubiquitous Cretaceous-age volcanic rocks that seem to blanket the Early Cretaceous and Jurassic basement of the western Pacific Ocean.

Site 800 in the Pigafetta Basin penetrated 56 m of massive alkali dolerite sills. $^{40}Ar/^{39}Ar$ laser analyses of mineral separates revealed a crystallization age of 126.1 ± 0.6 Ma. The isotopic composition of these dolerite sills shows a strong HIMU component (high radiogenic Pb, low radiogenic Sr), nearly identical to similar age lavas recovered from nearby seamounts. Both the sills and seamounts of the Pigafetta Basin are Early Cretaceous products of the South Pacific Isotopic and Thermal Anomaly (SOPITA), which is responsible for the ocean islands and thermal (?) swell found in the South Pacific today.

Site 801, drilled into the Jurassic Quiet Zone crust of the Pigafetta Basin, penetrated 131 m of basaltic flows divided into an upper sequence of alkalic basalts, an altered hydrothermal deposit, and a lower tholeiitic sequence. For the lower tholeiitic basalts, whole rock incremental- and laser-heating experiments revealed an age of 166.8 ± 4.5 Ma, almost exactly that predicted by simple linear extrapolation of the M-sequence magnetic lineation ages. The age and composition of the tholeiites offers important proof that the "Quiet Zone" crust of the western Pacific is indeed Jurassic mid-ocean ridge basalt (MORB), and not a product of mid-Cretaceous, intra-plate volcanic events.

For the upper alkalic basalts at Site 801, $^{40}Ar/^{39}Ar$ mineral incremental-heating and laser-fusion experiments yielded an age of 157.4 ± 0.5 Ma. About 10 m.y. younger than that predicted by extrapolation of the M-sequence anomalies, the alkalic basalts were erupted in an off-ridge environment, which is consistent with both the geochemistry of the basalts and the Bathonian to Callovian radiolarian age of the overlying sediments. The 157.4 Ma age also serves as an important calibration point on the Geologic Time Scale (GTS), but further work may be needed to verify the correlation of the radiolarian zonations in the Pacific with the time scale stages based on European sections.

Site 802 in the East Mariana Basin penetrated 51 m of basaltic pillow units and flows. Whole rock $^{40}Ar/^{39}Ar$ incremental-heating analysis of two samples revealed a crystallization age of 114.6 ± 3.2 Ma. Although the isotopic composition of these basalts indicates an ocean island basalt component, the major and trace element chemistry shows a strong MORB affinity. This is very similar to the contemporaneous basalts recovered at Site 462A in the Nauru Basin, and both seem more closely related to the formation of Ontong Java Plateau, ca. 120 Ma, rather than to products of the SOPITA.

INTRODUCTION

The principal goal of Ocean Drilling Program (ODP) Leg 129 was to recover the oldest rocks of the Pacific Ocean—a sedimentary section from the Mesozoic superocean and Jurassic ocean crust from the western Pacific. This goal, which had eluded nine previous legs over two decades of drilling by ODP and the Deep Sea Drilling Project, was finally achieved at Site 801 in the Pigafetta Basin. Sites 800 and 802 terminated in younger sill and flow complexes, products of mid-Cretaceous volcanism which almost ubiquitously blankets the oldest portions of the western Pacific.

The purpose of this study was to determine radiometric ages for the volcanic basement sampled at each of these sites. Before this study, no reliable radiometric ages for Jurassic or Early Cretaceous ocean crust from any ocean had been determined. In spite of the difficulty in determining concordant crystallization ages for altered ocean crust, reliable ages were determined for volcanic rocks from each of the sites studied here. Also, we report what may be the first reliable ages for tholeiitic, mid-ocean ridge basalt (MORB) of any age recovered during the more than two decades of ocean floor drilling.

The success of this study is due in large part to the recent advances in the $^{40}Ar/^{39}Ar$ geochronology of very small samples. The increased sensitivity of the new analytical systems allows one to work with datable mineral separates in quantities that previously would have been insufficient: 10–20 mg for plagioclase, less than 1 mg for more potassic phases such as biotite. Also, the greatly reduced analytical time necessary for the very small sample techniques—20 min. vs. 3 hr to 1 day per sample for previous systems—facilitates generating sets of age data required for applying internal concordance tests designed to distinguish reliable ages. Furthermore, much of the success in obtaining reliable results from whole rock samples can be attributed to careful petrographic selection of the least altered samples with the most holocrystalline groundmass.

SITE LOCATION AND SUMMARY

Hole 800A was drilled on magnetic anomaly M33 in the northwest Pigafetta Basin, 80 km to the northeast of Himu Seamount (Fig. 1). The oldest sediments recovered were earliest Cretaceous in age (Lancelot, Larson, et al., 1990), but the hole bottomed in 56 m (7 m recovery) of clearly intrusive, massive dolerite sills. The dolerites are clearly younger than the sedimentary rocks that they intrude, and the volcanic basement recovered at Hole 800A is probably closer in age to the thick sequence of mid-Cretaceous volcaniclastics recovered higher in the section than to the presumed Jurassic crust located somewhere below.

Site 801 was drilled 600 km to the southeast of Site 800, in the Jurassic Quiet Zone 450 km to the southeast of the oldest magnetic lineation identified in all of the ocean basins (anomaly M37). Holes 801B and 801C represent a composite section of more than 130 m of penetration into submarine basalts (Lancelot, Larson, et al., 1990). A 3 m thick hydrothermal deposit recovered at Hole 801C divides the

[1] Larson, R. L., Lancelot, Y., et al., 1992. *Proc. ODP, Sci. Results,* 129: College Station, TX (Ocean Drilling Program).

[2] U.S. Geological Survey, 345 Middlefield Rd., Menlo Park, CA 94025, U.S.A.

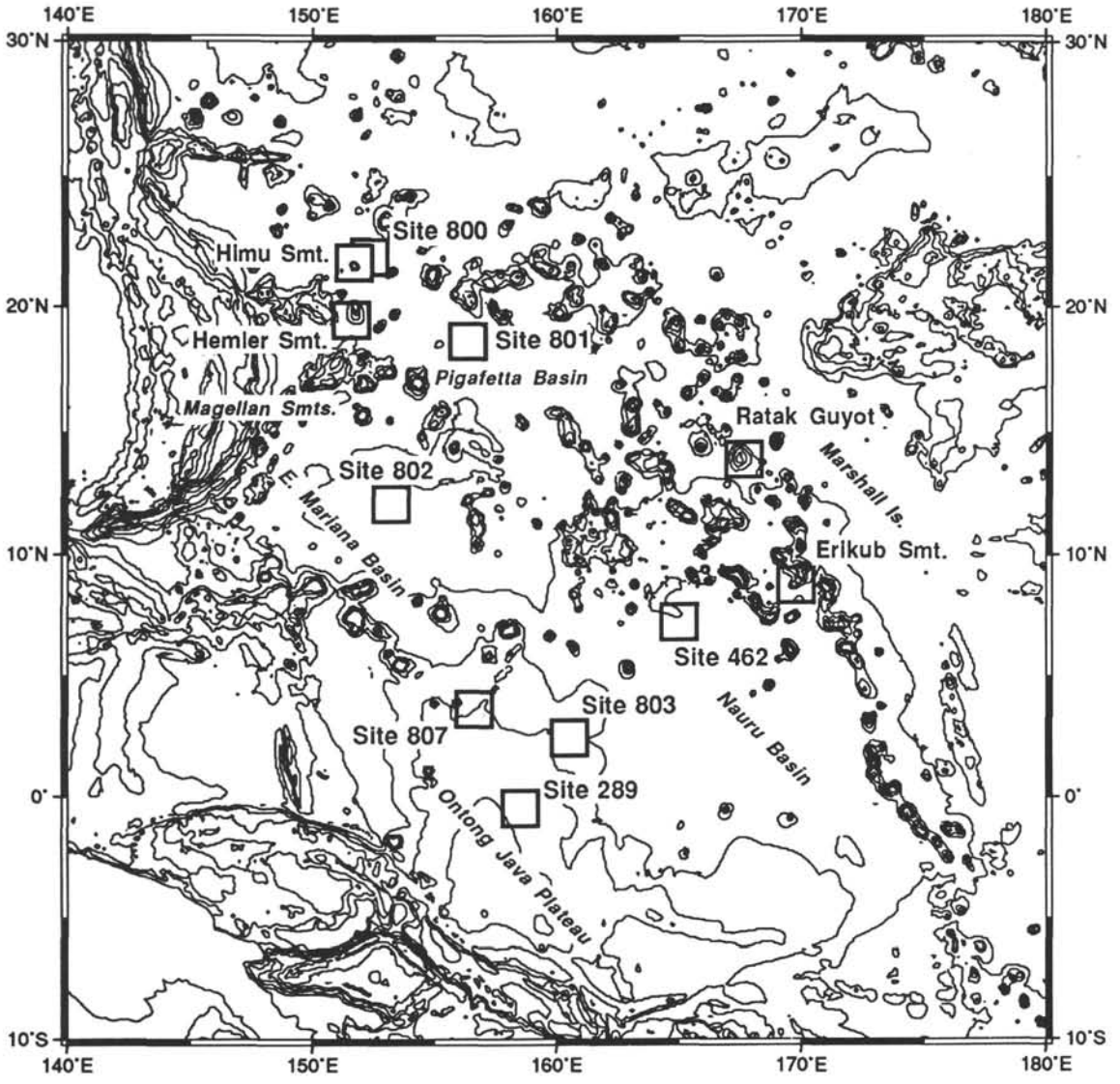

Figure 1. Sites of Mesozoic volcanism in the western Pacific for which both reliable $^{40}Ar/^{39}Ar$ ages and radiogenic isotope analyses are available, including Sites 800, 801, and 802 drilled during Leg 129. Figure drawn using the GMT utilities of Wessel and Smith (1991).

section into two distinct compositional groups: all of the cooling units at Hole 801B and the cooling units above the deposit at Hole 801C are alkalic basalts; all of the cooling units below the deposit at Hole 801C are tholeiitic, mid-ocean ridge basalts (Floyd et al., 1991; Floyd and Castillo, this volume). The oldest dated sediments are from the latest Bathonian or from the Bathonian-Callovian boundary (Matsuoka, this volume).

Site 802 was drilled in the East Mariana Basin, 400 km west of Ita Mai Tai Guyot (Fig. 1). A set of Mesozoic magnetic anomalies similar to those found in the Pigafetta Basin has been identified in the East Mariana Basin. However, the identification of the East Mariana Basin magnetic anomalies is less certain older than M33, and the magnetic age of the ocean crust near Site 802 can only be assigned tentatively to anomalies M35–M37 (Lancelot, Larson, et al., 1990). The oldest sediments recovered are younger than late Aptian, at least 40 m.y. younger than the magnetic anomaly age (Lancelot, Larson, et al., 1990). As at Site 800, the age of the recovered basement seems more closely related to the mid-Cretaceous volcaniclastics higher in the section than to the apparent Jurassic crust underneath.

K-Ar GEOCHRONOLOGY

The K-Ar clock, and especially the $^{40}Ar/^{39}Ar$ technique, has been widely used to date oceanic lavas. However, several fundamental assumptions of the technique may be violated by samples that have been altered in the submarine environment. Both addition of potassium and loss of radiogenic ^{40}Ar during alteration will lower the apparent K-Ar age, making conventional K-Ar apparent ages minimum estimates for the age of crystallization. $^{40}Ar/^{39}Ar$ total-fusion analyses have been used with some success on whole rock samples dredged from seamounts (for example, Clague et al., 1975; Dalrymple and Clague, 1976; Schlanger et al., 1984; Watts et al., 1988). For a $^{40}Ar/^{39}Ar$ total-fusion age of an altered volcanic rock to be accurate, radiogenic ^{40}Ar generated over geologic time and K-derived ^{39}Ar generated during irradiation must both be lost from alteration phases that are younger than the crystallization age. It seems that if the extent of alteration is relatively small, this loss is relatively complete, and a significant fraction of the original K-Ar system is undisturbed. For such samples, total-fusion ages can give reliable estimates of the crystallization age.

No independent criteria have been developed, however, to test whether a given sample is too altered for the $^{40}Ar/^{39}Ar$ total-fusion technique to yield an accurate age. Pringle (1992) has shown that, even for samples that are only partially disturbed (i.e., disturbed samples that still have concordant incremental-heating plateau), $^{40}Ar/^{39}Ar$ total-fusion ages can be as much as 10% too old or too young. Samples that do not have concordant incremental-heating plateau can easily have whole rock total-fusion ages ± 30% of the crystallization age, even if they have been chosen using petrographic criteria such as those proposed by Mankinen and Dalrymple (1972). Pringle (1992) has also shown that some total-fusion ages of carefully cleaned plagioclase mineral separates may not give reliable age estimates.

The real power of using $^{40}Ar/^{39}Ar$ geochronology in deciphering the crystallization age of altered rocks is that accurate crystallization ages can be differentiated from unreliable ages using a series of *internal* tests for a set of apparent ages from a given sample. It may not be possible to differentiate *why* a particular age from a sample is unreliable, although alteration is certainly a contributing factor. However, one can test *whether* the K-Ar clock of a particular sample is too disturbed to reveal a meaningful age.

The need for this internal consistency check is especially important for the relatively low-K, moderately to highly altered samples typical of those recovered from the ocean floor by ODP. Rocks with interstitial glass or very fine-grained groundmass—among the most common recovered from the ocean floor—do not give reliable ages, even when alteration products cannot be detected petrographically (Mankinen and Dalrymple, 1972; Fleck et al., 1977). In fact, Siedemann (1978) concluded that it would not be possible to reliably date any altered mid-ocean ridge basalt using the $^{40}Ar/^{39}Ar$ technique. This author is not aware of any previous study which has reliably dated such material, the recovery of which was one of the principal goals of Leg 129.

Criteria for Interpreting $^{40}Ar/^{39}Ar$ Apparent Ages

To test whether a sample can reveal a reliable $^{40}Ar/^{39}Ar$ age, one must first generate a set of ages upon which to apply the criteria presented below. Incremental-heating experiments can be used to generate an age spectrum, and the plateau steps can be tested with the criteria described below (for example, Dalrymple et al., 1980). A series of laser-fusion ages on mineral separates, whether degassed or simple total-fusion analyses, can also be tested. Davis et al. (1989) used a set of whole rock total-fusion ages from a seamount to determine that the group as a whole represented a concordant age for that seamount, even though each of the samples exhibited disturbed whole rock incremental-heating experiments indicative of significant internal argon redistribution. Below, we apply a new approach for samples that exhibit a significant amount of internal argon redistribution and loss, generating a mid-temperature (700°–1100°C) age for a series of small whole rock chips and applying the criteria below to that set.

Following Pringle (1992), we modify the conservative criteria of Lanphere and Dalrymple (1978) and Dalrymple et al. (1980) so that each of the criteria involves the use of a rigorous statistical test. We apply these criteria to the set of apparent ages for a given sample. We accept that this set of apparent ages represents an accurate estimate of the crystallization age of the sample only if:

1. No age difference can be detected between any of the individual ages at the 95% confidence level. For an incremental-heating experiment, these ages should represent a well-defined, high-temperature age plateau representing three or more contiguous steps which contain at least 50% of the ^{39}Ar released. For total-fusion analyses and ages from degassed phases, the selected ages should include over 50% of the ^{39}Ar released, making sure to count the degassing steps in the total amount of ^{39}Ar.

2. A well-defined isochron exists for the set; i.e., the F variate statistic for the regression is sufficiently small at the 95% confidence level.

3. The weighted mean age from the ages chosen in (1) and the isochron analysis of the data from (2) are not significantly different at the 95% confidence level.

4. The $^{40}Ar/^{36}Ar$ intercept from the isochron analysis in (2) is not significantly different from the atmospheric value of 295.5 at the 95% level.

For the test of a well-defined isochron in (2), most authors follow Brooks et al. (1972) and McIntyre et al. (1966), who suggest a general cutoff value of 2.5 for the ratio between scatter about the isochron to how much of that scatter can be explained within the limits of analytical error alone. This departs from standard practice in not using some level of significance to reject the model age, and does not take into consideration that different cutoff values should be used for different numbers of data points. The more rigorous F variate statistical test is preferred here. For example, the proper cutoff value at the 95% confidence level for isochrons with 4, 6, 8, and 11 data points is 3.00, 2.37, 2.10, and 1.88, respectively. If this ratio is exceeded, then there is more scatter about the isochron than can be explained by analytical error alone; i.e., some additional geologic or experimental disturbance is significant. Further justification of an age derived from such an isochron is necessary before that age can be accepted as having geological meaning.

Samples Studied

Site 800

Three cooling units of massive, medium-grained, aphyric alkalic dolerite were described by Lancelot, Larson, et al. (1990) from the 7 m of recovered material at Hole 800A (56 m total basement penetration). From thin section examination, it was determined that none of the samples were acceptable for whole rock analysis. Variable amounts of clay, carbonate, and other low temperature alteration phases replace between 20% and 60% of the original crystallization phases; some individual mineral grains are completely replaced. Samples from the lowermost unit appeared most suitable for mineral separates; two samples of slightly different mineralogy were chosen as the freshest and coarsest-grained fractions. Sample 129B-800-61R-1, 17–24 cm, is representative of most of the unit. It is dominated by zoned plagioclase laths 0.5 to 5.0 mm in diameter, many with altered cores, and subhedral titanaugite prisms 0.4 to 4 mm long. Sample 58R-2, 52–60 cm, from the top of the unit, is similar but also contains small but significant amounts of apparently primary potassium feldspar and hornblende as well as a trace of apparently secondary, fine-grained actinolite and biotite.

Site 801

Most of the cooling units at both Sites 801B and 801C were interpreted as relatively thin (0.5 to 4 m thick), aphyric basalt flows, although one unit in the tholeiitic section is unusually thick (c. 13.5 m, Lancelot, Larson, et al., 1990). Actual pillow lava margins, the most reliable indicator of extrusive igneous activity, were recovered only from some of the tholeiitic cooling units. For the alkalic cooling units, the bottommost unit at Hole 801B and several of the uppermost units at Hole 801C were clearly intrusive; they may in fact represent a single unit (Lancelot, Larson, et al., 1990). Although the other alkalic cooling units were interpreted as extrusive lava flows, no actual pillow margins were recovered. Thus, it is possible that at least some of the units could be thin, intrusive, basalt sills. If this were true, then the age of the alkalic basalts would be a minimum age for the "overlying" radiolarian-bearing sedimentary rocks, rather than a maximum age as is assumed in the discussion below.

None of the samples from the alkalic section of Site 801 were fresh enough for whole rock analysis, but two samples were selected for mineral separation. Sample 129B-801-1R-1, 109–119 cm, from the uppermost unit of Hole 801C is an aphyric, medium-grained, hypocrystalline basalt. It correlates to two units at Hole 801B (units 6 and 7). Matrix plagioclase, partially replaced by white clays, ranged up to 1 or 2 mm in diameter and was coarse enough to separate. Also, we were able to separate about a milligram of fine-grained biotite flakes, 0.1 to 0.15 mm in diameter, which grew as a late-stage yet primary igneous phase. Sample 44R-3, 13–22 cm, has 5%–10% subhedral plagioclase phenocrysts up to 2 mm in diameter in a glassy groundmass; it is from the intrusive unit at the bottom of Hole 801B, and correlates to two units at Hole 801C (units 4 and 6).

Most of the cooling units of the tholeiitic section of Site 801 are hypocrystalline to cryptocrystalline, aphyric basalts with groundmass containing 10%–50% smectitic clays. Samples from these units are too glassy or altered for whole rock analysis and too fine-grained for mineral separates. Several of the less-altered, coarser-grained flow interiors were sampled for whole rock $^{40}Ar/^{39}Ar$ analysis, but none gave any useful age information. Only the two samples selected from the interior of the thick flow gave concordant results. Both samples—10R-5, 53–58 cm, and 10R-6, 21–26 cm—are fine-grained yet holocrystalline, aphyric basalts with only a few percent of green smectite after glass in an intersertal groundmass.

Sample 801C-5R3, 35–38 cm, contained 5% to 10% plagioclase phenocrysts 1 to 4 mm in diameter in a highly altered, hypocrystalline groundmass. We were able to separate and carefully acid clean about 30 mg of relatively clean plagioclase. However, we could not get any useful age information using either the laser or resistance furnace systems described below, presumably because of the low potassium content of the separate (<.01%), the effects of alteration not visible in the mineral separate, or both.

Site 802

Almost 17 m of pillow basalts and thin flows representing 51 m of basement penetration at Hole 802A were divided into 17 cooling units (Lancelot, Larson, et al., 1990). The upper 16 units are relatively thin, less than 1.5 m thick, hypocrystalline basalt with abundant quench textures, too fine-grained and glassy for $^{40}Ar/^{39}Ar$ geochronology in spite of the low degree of alteration apparent in most of the samples. The bottommost unit was interpreted as a 3 m thick flow and is similar to the other flows except that it grades into a fine-grained yet holocrystalline groundmass in the center, with only a few percent of green clays after olivine microphenocryts and a trace of carbonate in some areas. Both samples selected for $^{40}Ar/^{39}Ar$ whole rock incremental-heating experiments were from this unit.

Techniques

Samples for mineral separation were crushed by hand in a hardened-steel mortar and pestle. Conventional heavy liquid and magnetic techniques were used to prepare pure mineral separates, which were further cleaned with appropriate acids in a 40Khz ultrasonic bath. Feldspar was cleaned with cold 5%–10% HF and warm 2.5N HCl. Hornblende was cleaned with warm 2.5N HCl. Biotite was not cleaned in any acid, but was carefully hand-picked of impurities. Whole rock samples were prepared as 6 mm diameter cores drilled from the freshest sections of 1 cm thick slabs of the basalt.

The whole rock cores, 0.5–0.8 g, and mineral separates, 1–15 mg encapsulated in Cu foil packets, were sealed in fused-silica vials and irradiated for 24 to 40 hours in the core of the Geological Survey TRIGA reactor (Dalrymple et al., 1981). The samples were closely monitored with sanidine separated from the 27.92 Ma Taylor Creek Rhyolite (sample 85G003 of Dalrymple and Duffield, 1988). The neutron flux parameter, J, was calculated from multiple analyses of Taylor Creek sanidine monitors using the U.S. Geological Survey (USGS) laser system, and is reproducible to better than 0.3%. Six packets of the hornblende standard Mmhb-1 were analyzed as unknowns during this study and gave an average age of 514.0 ± 1.4 Ma (standard error of the mean).

Three different extraction systems and mass spectrometers were used for this study. The first system, at the USGS in Menlo Park, CA, is the GLM (Great Little Machine) continuous laser extraction system described by Dalrymple (1989). It employs an ultrasensitive, ultraclean mass spectrometer capable of measuring the very small (0.1–15 mg) samples available for most of this study. It also includes an infrared microscope for measuring the temperature of samples during laser-heating. Most of the analyses reported here were analyzed on the GLM. The second system, at Stanford University, is similar to the USGS laser system but also has an all-metal Staudacher-type resistance furnace attached to the cleanup system. This system was used for two incremental-heating experiments on plagioclase. The third system, at the USGS, also has an all-metal resistance furnace for incremental-heating but is attached to a Nier-type single-collector mass spectrometer and is about two orders of magnitude less sensitive than the first two systems. The third system was used for incremental-heating experiments on the 6 mm diameter whole rock cores.

Mean ages were calculated as weighted means, where each age is weighted by the inverse of their variance (Taylor, 1982). Incremental-heating experiments were reduced as both age spectra and isochrons. Isochron ages were calculated for both $^{40}Ar/^{36}Ar$ vs. $^{40}Ar/^{39}Ar$ and $^{36}Ar/^{40}Ar$ vs. $^{39}Ar/^{40}Ar$ correlation diagrams using the York2 least-squares cubic fit with correlated errors (York, 1969); SUMS/N-2 is the F variate statistic for this regression. Dalrymple et al. (1988) found no significant difference between the two correlations when the error correlation coefficients are determined using the method recommended by York (as quoted in Ozima et al., 1977).

RESULTS

The $^{40}Ar/^{39}Ar$ age determinations for basaltic basement recovered at Sites 800, 801, and 802 during Leg 129 are summarized in Table 1; the individual age determinations are shown in Tables 2, 3, 4, and 5. The best age for each site is the weighted mean of the isochron ages for each of the experiments described below. We prefer to use the isochron age as the best estimate of each sample age because it (1) combines both an estimate of the degree of internal discordance - the scatter about the isochron line - and an estimate of analytical error in the final error estimate, and (2) makes no assumption about the composition of the initial non-radiogenic, or trapped, argon component.

Figure 2, a time calibration plot of the Mesozoic magnetic anomalies and the preceding Jurassic Quiet Zone, summarizes the age of the ocean crust recovered during Leg 129. It includes both the radiometric ages determined here and the biostratigraphic ages determined from the ages of the oldest sedimentary rocks overlying the basalt (Lancelot, Larson, et al., 1990; Matsuoka, this volume). Note that all of the ocean crust ages in Figure 2 except for the Leg 129 results are biostratigraphic; i.e., no reliable radiometric ages for Jurassic or Early Cretaceous ocean crust from any ocean were available before this study.

Hole 800A

Two $^{40}Ar/^{39}Ar$ experiments were done on the mineral separates from the alkalic dolerites of Site 800. The first was a laser incremental-heating experiment using a defocussed laser beam on the K-feldspar from 800A-52R-2, 52–60 cm. It revealed a concordant high temperature plateau over almost 80% of the gas released; the isochron analysis was also concordant (Fig. 3A, Table 1). The second was a series of mineral laser fusion analyses conducted on plagioclase from Sample 61R-1, 17–24 cm and on plagioclase, K-feldspar, and hornblende from Sample 52R-2, 52–60 cm (Table 2). The isochron with all of the

Table 1. Summary of Leg 129 radiometric ($^{40}Ar/^{39}Ar$) age determinations.

Sample	Material	Plateau or weighted TF age: ^{39}Ar (%)	Plateau or weighted TF age: Age ± 1 s.d.	Isochron age: Age ± 1 s.d.	Isochron age: $^{40}Ar/^{36}Ar_i$ ± 1 s.d.	SUMS/N-2	N
Site 800			[a]Best age:	126.1 ± 0.6 Ma			
800A-52R-2, 52–60 cm, and 61R-1, 17–24 cm	Plagioclase and K-feldspar	[b]100	126.1 ± 0.6 Ma	126.1 ± 0.7 Ma	279.1 ± 42.0	2.16	20
800A-52R-2, 52–60 cm	K-feldspar	79.7	125.8 ± 0.7 Ma	126.1 ± 0.9 Ma	148.2 ± 71.4	1.30	11
Site 801	**Alkalic basalts**		[a]Best age:	157.4 ± 0.5 Ma			
801B-44R-3, 13–22 cm	Plagioclase	[b]68.9	158.1 ± 0.5 Ma	158.1 ± 0.7 Ma	295.0 ± 4.3	0.31	5
	Plagioclase	50.3	155.0 ± 1.0 Ma	154.1 ± 2.6 Ma	305.1 ± 26.8	0.06	4
801C-1R-1, 109–119 cm	Plagioclase	[b]100	157.6 ± 0.8 Ma	157.9 ± 1.4 Ma	233.2 ± 170.7	0.95	6
	Biotite	[b]100	161.5 ± 0.9 Ma	159.7 ± 2.1 Ma	313.9 ± 18.9	0.83	6
	Plagioclase	98.0	156.2 ± 0.8 Ma	156.2 ± 0.8 Ma	287.3 ± 17.6	0.40	8
	Tholeiitic basalts		[a]Best age:	166.8 ± 4.5 Ma			
801C-10R-5, 53–58 cm	Basalt core	59.4	158.6 ± 2.7 Ma	153.7 ± 8.0 Ma	366.7 ± 108.9	0.03	4
801C-10R-6, 21–26 cm	Basalt chips	[c]62.4	171.5 ± 1.1 Ma	173.0 ± 5.5 Ma	285.7 ± 30.9	1.58	9
Site 802			[a]Best age:	114.6 ± 3.2 Ma			
802A-62R-2, 45–50 cm	Basalt core	78.4	118.3 ± 1.6 Ma	116.8 ± 4.8 Ma	303.2 ± 39.4	2.12	4
	Basalt core	100.0	114.7 ± 2.8 Ma	112.5 ± 4.6 Ma	306.0 ± 24.5	0.40	6
802A-62R-3, 4–12 cm	Basalt core	90.5	115.8 ± 2.6 Ma	116.0 ± 13.1 Ma	294.4 ± 38.3	0.97	4

[a]"Best age" is calculated by weighting the individual isochron ages by the inverse variance.
[b]Laser total-fusion analyses, including fusions of previously degassed minerals.
[c]"Plateau" steps from individual basalt fragments heated to about 1100° after degassing at 600° and 700°.

feldspar laser fusion data (n = 20) is shown in Figure 3B. Note that the F variate statistic for the isochron, 2.16, is slightly greater than would be expected from analytical error alone. This extra scatter is included in the calculation of the estimate of the reported error in age. The hornblende apparent ages, ca. 125 Ma, were slightly younger than the rest of the mineral data and had significantly lower radiogenic ^{40}Ar compositions (Table 2), apparently because of a small amount of secondary actinolite that could not be easily separated from the hornblende. Inclusion of these data in the isochron analysis resulted in a slightly higher isochron age and lower initial $^{40}Ar/^{36}Ar$ intercept, similar to the example given by Lanphere and Dalrymple (1978). Their conclusion not to include such data in the final age analysis is followed here. The best age for the Hole 800A dolerite sills is the weighted mean age of these two experiments, 126.1 ± 0.6 Ma.

Site 801 Alkalic Basalts

Five different experiments were done on three different phases from the two units studied here; all meet or exceed the reliability criteria. Incremental-heating experiments using the Stanford resistance furnace were conducted on plagioclase from each of two units. Sample 801C-1R-1, 109–119 cm showed no signs of disturbance (Fig. 4A). Sample 801B-44R-3, 13–22 cm, showed young apparent ages at both low and high temperatures, probably due to ^{40}Ar loss from alteration phases and Ar redistribution mechanisms, respectively, but did show a good mid-temperature plateau for almost 60% of the ^{39}Ar released (Fig. 4B). Three sets of laser fusion analyses, including co-existing biotite and plagioclase from Sample 801C-1R-1, 109–119 cm, also revealed concordant ages (Figs. 4C, D, E). The best age for the alkalic basalts at Site 801 is the weighted mean age of all five experiments, 157.4 ± 0.5 Ma.

Hole 801C Tholeiitic Basalts

The two samples chosen from the 13.5 m thick flow were the only samples from tholeiitic sequence from Hole 801C that yielded concordant age information according to the criteria described above. Both samples exhibited a disturbed age spectrum typical of argon redistribution (Fig. 5). Fine-grained, altered whole rock samples are very susceptible to argon redistribution that has been attributed mainly to the recoil of ^{39}Ar from higher-potassium sites degassed at low temperatures to lower-potassium sites degassed at high temperatures. This results in an age spectrum with a decreasing step-like pattern such as those found in Figures 5 and 6. The six-step incremental-heating experiment on Sample 801C-10R-5, 53–58 cm, revealed a mid-temperature plateau with 59.4% of the ^{39}Ar released (Fig. 5A).

For Sample 801C-10R-6, 21–26 cm, a new approach of determining concordant ages from rocks with suspect argon redistribution profiles was tested. Because samples with such problems will reveal mid-temperature plateaus when they are concordant, the mid-temperature release was extracted from nine individual chips weighing 2–5 mg each (Fig. 5B). Using an infrared microscope to monitor the temperature of the chips during heating, the chips were degassed at 600°C and 700°C and the liberated argon was combined and measured for each temperature. Next, each chip was heated to 1100°C, and the gas released was measured for each chip. Finally, the chips were fused in three groups of three chips each and the gas for each group was measured. The 1100°C steps included 62% of the ^{39}Ar released (Fig. 5B); the isochron and age spectrum are concordant (Table 1). The best age for the tholeiites at Hole 801C is the weighted mean isochron age for this experiment and the incremental-heating experiment described above, 166.8 ± 4.5 Ma.

Hole 802A

The three whole rock incremental-heating experiments on samples from the thickest, most holocrystalline flow from Hole 802A all showed typical argon redistribution profiles (Fig. 6). Each experiment was concordant according to the criteria used for this study, with ca. 80%, 100%, and 90% of the ^{39}Ar released on the age plateaus. The best age for the lowermost flow from Hole 802A is the weighted mean age of the isochron ages, 114.3 ± 3.2 Ma.

Table 2. Incremental heating and laser fusion data for mineral separates from Hole 800A dolerites.

Step	$^{40}Ar/^{39}Ar$[a]	$^{37}Ar/^{39}Ar$[a]	$^{36}Ar/^{39}Ar$[a]	$^{40}Ar_R$[b]	$^{40}Ar_K$[b]	$^{39}Ar_{Ca}$[b]	$^{36}Ar_{Ca}$[b]	K/Ca	^{39}Ar (%)	Apparent age[c] (Ma)
800A-61R-1, 17–24 cm			Mineral TF		$J = 0.011675$				Total gas age =	125.98 ± 0.61
Plag	6.403	3.052	0.001584	96.4	0.1	0.2	51.8	0.160	4.1	125.75 ± 0.39
Plag	6.329	3.311	0.001410	97.5	0.1	0.2	63.2	0.148	8.1	125.73 ± 0.37
Plag	6.371	3.356	0.001537	97.0	0.1	0.2	58.7	0.146	1.3	125.90 ± 0.60
[d]Plag	6.295	3.075	0.001089	98.7	0.1	0.2	75.9	0.159	4.6	126.55 ± 0.38
[d]Plag	6.285	3.329	0.001174	98.6	0.1	0.2	76.2	0.147	4.2	126.27 ± 0.39
[d]Plag	6.279	3.426	0.001212	98.5	0.1	0.2	76.0	0.143	3.8	126.09 ± 0.39
800A-58R-2, 52–60 cm			Mineral TF		$J = 0.011675$					
Plag	6.332	1.7879	0.000929	97.8	0.1	0.1	51.8	0.274	2.4	126.09 ± 0.44
Plag	6.308	1.0728	0.000676	98.1	0.1	0.1	42.7	0.456	4.3	125.90 ± 0.38
Plag	6.322	1.7037	0.000868	98.0	0.1	0.1	52.8	0.287	6.1	126.11 ± 0.37
Plag	6.309	1.6377	0.000800	98.2	0.1	0.1	55.0	0.299	4.0	126.14 ± 0.39
Plag	6.205	1.1759	0.000483	99.1	0.1	0.1	65.5	0.416	4.1	125.17 ± 0.38
[d]Plag	6.273	1.4479	0.000554	99.1	0.1	0.1	70.4	0.338	9.1	126.54 ± 0.36
[d]Plag	6.270	1.4223	0.000607	98.8	0.1	0.1	63.0	0.344	8.4	126.14 ± 0.36
[d]Plag	6.286	1.3811	0.000567	99.0	0.1	0.1	65.5	0.354	4.5	126.62 ± 0.38
[d]Plag	6.283	1.2215	0.000526	99.0	0.1	0.1	62.4	0.401	5.7	126.52 ± 0.37
Kspar	6.307	0.12143	0.000367	98.3	0.1	0.0	8.9	4.03	1.6	126.12 ± 0.53
Kspar	6.249	0.09529	0.000125	99.4	0.1	0.0	20.4	5.14	2.5	126.33 ± 0.43
Kspar	6.252	0.16390	0.000240	99.0	0.1	0.0	18.4	2.99	2.3	125.84 ± 0.44
Kspar	6.201	0.10669	0.000296	98.6	0.1	0.0	9.7	4.59	3.3	124.42 ± 0.40
Kspar	6.291	0.15418	0.000150	99.4	0.1	0.0	27.7	3.18	2.9	127.12 ± 0.41
Hbl	8.250	4.969	0.008546	74.1	0.1	0.3	15.6	0.098	2.3	124.77 ± 0.55
Hbl	8.048	5.750	0.007902	76.6	0.1	0.4	19.6	0.085	2.1	125.82 ± 0.56
Hbl	8.942	6.621	0.011340	68.3	0.1	0.4	15.7	0.074	3.2	124.86 ± 0.57
Hbl	7.964	6.322	0.007848	77.1	0.1	0.4	21.7	0.077	2.7	125.42 ± 0.52
Hbl	8.065	5.124	0.007956	75.8	0.1	0.3	17.3	0.095	2.2	124.82 ± 0.55
800A-58R-2, 52–60 cm			K-feldspar IH		$J = 0.01166$				Total gas age =	125.76 ± 0.63
[e]0.5W	6.543	0.16631	0.001879	91.6	0.1	0.0	2.3	2.95	6.1	121.90 ± 0.60
0.8W	6.275	0.15987	0.000313	98.6	0.1	0.0	13.5	3.06	7.2	125.70 ± 0.53
1.0W	6.121	0.13494	0.000364	98.3	0.1	0.0	9.8	3.63	7.0	122.34 ± 0.54
1.3W	6.284	0.11345	0.000178	99.2	0.1	0.0	16.9	4.32	9.6	126.60 ± 0.46
1.6W	6.306	0.11740	0.000574	97.4	0.1	0.0	5.4	4.17	3.0	124.74 ± 1.03
2.0W	6.294	0.11575	0.000036	99.9	0.1	0.0	83.9	4.23	5.0	127.62 ± 0.68
2.4W	6.289	0.11844	0.000075	99.7	0.1	0.0	41.6	4.14	4.0	127.30 ± 0.80
3.0W	6.297	0.12040	0.000592	97.3	0.1	0.0	5.4	4.07	5.7	124.45 ± 0.61
3.6W	6.299	0.10882	0.000234	98.9	0.1	0.0	12.3	4.50	3.3	126.55 ± 0.94
4.2W	6.290	0.12195	0.000387	98.2	0.1	0.0	8.3	4.02	3.9	125.52 ± 0.81
5.0W	6.285	0.12014	0.000542	97.5	0.1	0.0	5.9	4.08	4.6	124.51 ± 0.72
6.0W	6.313	0.11560	0.000328	98.5	0.1	0.0	9.3	4.24	13.0	126.30 ± 0.42
Fuse #1	6.321	0.10139	0.000303	98.6	0.1	0.0	8.8	4.83	17.1	126.57 ± 0.39
Fuse #2	6.330	0.14886	0.000180	99.2	0.1	0.0	21.8	3.29	10.7	127.53 ± 0.45

[a]Corrected for ^{37}Ar and ^{39}Ar decay, half-lives are 35.1 days and 259 years, respectively.
[b]Subscripts indicate radiogenic (R), calcium-derived (Ca), and potassium-derived (K) argon.
[c]Lambda E = 0.581E-10/yr, Lambda B = 4.692E-10/yr. Errors are standard deviaton of analytical precision.
[d]For these analyses, the samples were previously degassed with a 4W, 5-mm-wide laser beam.
[e]Laser power used for each of these steps, actual temperature was not measured.

DISCUSSION

Site 800

The age of the alkalic dolerite at Hole 800A is significantly younger than both the age inferred from the magnetization of the ocean crust and the age of the oldest overlying sediments (Fig. 2). This confirms the conclusion of Lancelot, Larson, et al. (1990) that the 800A dolerites are sills intruded into older sediments and are not related to the formation of the original ocean crust, presumably located somewhere below the recovered section.

The 126 Ma age is similar to the 120 Ma age for the alkalic basalts dredged from Himu Seamount, located 80 km to the southwest (Smith et al., 1989). The isotopic compositions of the 800A dolerites have a strong HIMU component (high radiogenic Pb, low radiogenic Sr), nearly identical to lavas recovered from Himu Seamount 80 to the southwest, Golden Dragon Seamount 150 km to the southeast, and two 80–90 Ma seamounts in the Marshall Islands (Castillo et al., this volume; Staudigel et al., 1991; Smith et al., 1989; Davis et al., 1989). Using the hotspot frame of reference, sites of Mesozoic volcanism in the western Pacific can be backtracked to the original location where they formed (Fig. 7). All four sites of Mesozoic volcanism with a HIMU isotopic signature (solid circles and squares) backtrack to the general vicinity of the Austral-Cook Islands. Three out of the four locations are indistinguishable from the present day location of the Rurutu hotspot, which has erupted lavas with a HIMU isotopic component.

Summarizing the unusual geochemical and geophysical characteristics of the modern day volcanism of islands and seamounts of the south central Pacific, Smith et al. (1989) and Staudigel et al. (1991) defined the South Pacific Isotopic and Thermal Anomaly (SOPITA, Fig. 7). They concluded that this anomalous region of the Pacific Basin was also responsible for at least some of the Cretaceous seamount volcanism of the western Pacific, and extended back to at least 120 Ma. With the new data from Site 800, we extend this back

Table 3. Incremental heating and laser fusion data for mineral separates from Site 801 alkalic basalts.

Step	$^{40}Ar/^{39}Ar$[a]	$^{37}Ar/^{39}Ar$[a]	$^{36}Ar/^{39}Ar$[a]	$^{40}Ar_R$[b]	$^{40}Ar_K$[b]	$^{39}Ar_{Ca}$[b]	$^{36}Ar_{Ca}$[b]	K/Ca	^{39}Ar (%)	Apparent age[c] (Ma)
801B-44R-3, 13–22 cm			Plagioclase IH		J = 0.004091				Total gas age =	148.4 ± 1.9
[d]630	44.49	21.90	0.09338	41.9	0.0	1.5	6.3	0.022	27.8	134.4 ± 6.3
690	26.38	22.69	0.02220	81.9	0.0	1.5	27.5	0.021	17.4	155.1 ± 1.3
750	25.65	22.94	0.019854	84.2	0.0	1.5	31.1	0.021	17.6	155.0 ± 1.1
800	23.31	23.48	0.012342	92.3	0.0	1.6	51.2	0.021	8.9	154.5 ± 1.5
890	25.95	20.88	0.019722	83.9	0.0	1.4	28.5	0.023	6.3	156.0 ± 2.6
980	24.54	21.04	0.016691	86.7	0.0	1.4	33.9	0.023	14.6	152.6 ± 1.0
1100	32.32	15.09	0.04400	63.5	0.0	1.0	9.2	0.032	7.3	146.8 ± 2.0
			Plagioclase TF		J = 0.004091				Total gas age =	153.7 ± 1.4
Degas 1	217.6	22.22	0.6760	9.0	0.0	1.5	0.9	0.022	22.5	140.9 ± 5.9
Fuse 0	26.08	22.95	0.019720	84.6	0.0	1.5	31.3	0.021	11.6	158.3 ± 0.7
Fuse 1	26.33	21.66	0.02034	83.7	0.0	1.5	28.7	0.022	22.0	157.9 ± 0.6
Degas 2	23.90	23.07	0.012255	92.5	0.0	1.5	50.7	0.021	11.5	158.5 ± 0.7
Fuse 2	33.56	21.33	0.04470	65.7	0.0	1.4	12.8	0.023	9.3	157.9 ± 0.9
Degas 3	23.30	23.26	0.010669	94.4	0.0	1.6	58.7	0.021	13.6	157.7 ± 0.6
Fuse 3	32.33	20.47	0.04293	65.8	0.0	1.4	12.8	0.024	9.5	152.4 ± 0.9
801C-1R-1, 109–119 cm			Plagioclase IH		J = 0.009419				Total gas age =	156.4 ± 0.9
[d]610	10.753	10.428	0.006488	89.8	0.1	0.7	43.2	0.047	1.2	158.1 ± 3.7
690	9.867	10.933	0.003950	96.9	0.1	0.7	74.5	0.044	5.4	156.7 ± 1.1
760	9.602	15.502	0.004580	98.7	0.1	1.0	91.0	0.031	35.8	155.8 ± 1.3
820	9.625	13.237	0.003806	99.2	0.1	0.9	93.6	0.037	21.7	156.6 ± 0.7
900	9.740	7.057	0.002417	98.4	0.1	0.5	78.5	0.069	11.9	156.6 ± 0.5
970	9.738	5.271	0.002057	98.0	0.1	0.4	68.9	0.093	8.1	155.8 ± 0.8
1070	10.075	7.948	0.004033	94.4	0.1	0.5	53.0	0.061	8.2	155.5 ± 0.6
1170	10.076	11.324	0.004762	94.9	0.1	0.8	64.0	0.043	4.7	156.7 ± 1.5
1330	12.430	16.136	0.014343	76.2	0.1	1.1	30.3	0.030	2.3	155.7 ± 3.2
1490	23.39	19.753	0.04638	48.1	0.0	1.3	11.5	0.024	0.8	184.0 ± 10.0
			Plagioclase TF		J = 0.01146				Total gas age =	157.7 ± 0.8
T. Fuse	8.023	12.802	0.003650	98.9	0.1	0.9	92.6	0.038	6.3	158.2 ± 1.0
"	8.041	12.623	0.003706	98.6	0.1	0.8	89.9	0.038	10.5	158.0 ± 0.7
"	8.052	14.286	0.004008	99.1	0.1	1.0	94.1	0.034	8.7	159.1 ± 0.8
"	8.024	14.088	0.004264	97.9	0.1	0.9	87.2	0.034	6.5	156.8 ± 1.0
"	8.010	13.578	0.003861	98.9	0.1	0.9	92.8	0.036	16.8	158.0 ± 0.6
Degas @ 4W	7.980	13.215	0.003875	98.5	0.1	0.9	90.0	0.037	31.4	156.8 ± 0.5
Fuse	8.013	11.665	0.003409	98.7	0.1	0.8	90.3	0.042	19.7	157.6 ± 0.5
			Biotite TF		J = 0.011460				Total gas age =	161.5 ± 0.9
T. Fuse	10.159	0.2275	0.006635	80.8	0.1	0.0	0.9	2.15	28.8	162.1 ± 0.8
"	9.252	0.14662	0.003386	89.2	0.1	0.0	1.1	3.34	8.7	163.0 ± 1.9
"	8.978	0.15729	0.002541	91.7	0.1	0.0	1.6	3.12	10.9	162.5 ± 1.5
"	8.913	0.16053	0.002887	90.5	0.1	0.0	1.5	3.05	8.1	159.4 ± 2.0
"	9.352	0.10005	0.004190	86.8	0.1	0.0	0.6	4.90	21.3	160.3 ± 1.2
"	9.686	0.2053	0.005276	84.0	0.1	0.0	1.0	2.39	22.1	160.7 ± 1.2

[a]Corrected for ^{37}Ar and ^{39}Ar decay, half-lives are 35.1 days and 259 years, respectively.
[b]Subscripts indicate radiogenic (R), calcium-derived (Ca), and potassium-derived (K) argon.
[c]Lambda E = 0.581E-10/yr, Lambda B = 4.692E-10/yr. Errors are standard deviation of analytical precision.
[d]Temperature of each incremental heating step (°C) using a resistance furnace for heating.

to at least 126 Ma, and conclude that all of the seamounts and sills of the Pigafetta Basin that have been studied to date are Early Cretaceous products of the same anomaly which is responsible for the ocean islands and thermal (?) swell found in the South Pacific today.

Site 801

Two of the most important scientific objectives of Leg 129 were to test the assumption of linear spreading rates and tectonics for the Jurassic Pacific crust, and to calibrate the oldest M-sequence magnetic anomalies. Figure 2 shows that the 166.8 Ma age for the tholeiitic ocean crust at Site 801 is almost exactly the age predicted for the ocean floor by simple linear extrapolation of the ages of the M-sequence magnetic lineations using the time scale of Harland et al. (1990). Major element, trace element, and isotope geochemistry of the 801 tholeiites are indistinguishable from those of modern MORB (Floyd et al., 1991; Floyd and Castillo, this volume; Castillo et al., this volume). Both the age and geochemistry of the basalts offer important proof that the quiet zone crust of the western Pacific is indeed Jurassic mid-ocean ridge basalt, and is not a product of mid-Cretaceous volcanic events.

Since this site was located in the Jurassic Quiet Zone, 450 km beyond the oldest indentified magnetic lineations (Fig. 2; Lancelot, Larson, et al., 1990), we can not directly calibrate the age of the M-sequence lineations. Also, the Site 801 tholeiite age is not precise enough for a useful calibration of the time scale. However, a simple linear extrapolation of the M25–M37 magnetic lineations found in the western Pigafetta Basin is consistent with the Harland et al. (1990) Geologic Time Scale (GTS) and offers indirect confirmation of the age of that sequence. This confirmation is extremely important, since the oldest well-dated magnetic lineation in the western Pacific is M9, dated at Hauterivian at DSDP Site 304 (Fig. 2).

Table 4. Incremental heating and laser fusion data for whole-rock samples from Site 801 tholeiitic basalts.

Step	$^{40}Ar/^{39}Ar$[a]	$^{37}Ar/^{39}Ar$[a]	$^{36}Ar/^{39}Ar$[a]	$^{40}Ar_R$[b]	$^{40}Ar_K$[b]	$^{39}Ar_{Ca}$[b]	$^{36}Ar_{Ca}$[b]	K/Ca	^{39}Ar (%)	Apparent age[c] (Ma)
801C-10R-5, 53–58 cm			Basalt core		$J = 0.004584$				Total gas age =	164.1 ± 2.0
600	33.82	27.20	0.04691	65.4	0.0	1.8	15.6	0.0177	35.0	177.2 ± 1.3
700	24.04	46.15	0.02667	82.4	0.0	3.1	46.5	0.0103	16.3	161.6 ± 4.8
800	21.92	32.42	0.016911	88.9	0.0	2.2	51.6	0.0148	14.0	157.7 ± 5.6
900	20.81	51.73	0.019575	91.9	0.0	3.5	71.1	0.0091	22.1	156.8 ± 3.8
1000	18.046	280.3	0.08043	91.7	0.1	18.8	93.8	0.0014	7.0	161.2 ± 11.4
1400	16.281	366.3	0.10975	79.6	0.1	24.5	89.8	0.0010	5.6	136.7 ± 14.5
801C-10R-6, 21–26 cm			Basalt		$J = 0.009995$				Total gas age =	175.8 ± 1.1
[d]600	39.26	14.855	0.09527	31.3	0.0	1.0	4.2	0.033	7.1	210.9 ± 4.8
[d]700	16.422	20.59	0.02257	69.3	0.1	1.4	24.5	0.023	14.5	196.9 ± 1.9
[e]1100:										
#1	12.648	36.18	0.018797	78.8	0.1	2.4	51.8	0.0132	4.1	175.3 ± 2.8
#2	13.488	33.53	0.02097	73.7	0.1	2.2	43.0	0.0143	7.3	174.7 ± 2.1
#3	11.773	45.86	0.018962	83.3	0.1	3.1	65.1	0.0104	7.4	173.8 ± 2.1
#4	12.723	40.68	0.02106	76.4	0.1	2.7	52.0	0.0117	9.4	171.8 ± 1.9
#5	12.843	40.69	0.02150	75.6	0.1	2.7	50.9	0.0117	9.3	171.6 ± 1.9
#6	12.563	44.58	0.02209	76.2	0.1	3.0	54.3	0.0107	5.3	169.6 ± 2.4
#7	12.523	37.82	0.019950	76.9	0.1	2.5	51.0	0.0126	8.5	169.8 ± 1.9
#8	12.849	39.86	0.02190	74.2	0.1	2.7	49.0	0.0120	6.2	168.6 ± 2.2
#9	13.316	39.95	0.02351	71.6	0.1	2.7	45.7	0.0119	4.9	168.5 ± 2.4
[f]Fuse:										
#1–#3	12.329	149.55	0.05449	65.8	0.1	10.0	73.8	0.0029	4.8	155.6 ± 4.5
#4–#6	11.659	144.92	0.05030	71.2	0.1	9.7	77.5	0.0031	6.1	158.7 ± 4.2
#7–#9	11.735	176.75	0.05982	69.0	0.1	11.8	79.5	0.0024	5.2	158.5 ± 5.1

[a]Corrected for ^{37}Ar and ^{39}Ar decay, half-lives are 35.1 days and 259 years, respectively.
[b]Subscripts indicate radiogenic (R), calcium-derived (Ca), and potassium-derived (K) argon.
[c]Lambda E = 0.581E-10/yr, Lambda B = 4.692E-10/yr. Errors are standard deviation of analytical precision.
[d]Degas 9 basalt fragments, each weighing between 2 and 5 mg, at 600° and then 700°C.
[e]Heat each of the previously heated basalt fragments to 1100°C, measure individually.
[f]Fuse previously heated basalt fragments, measure in three groups of three fragments each.

Harland et al. (1990) concluded that just a few biostratigraphically controlled, high quality isotopic ages from the Late Jurassic could greatly reduce the errors in the ages of the M-sequence magnetic anomalies. Thus, the 157.4 ± 0.5 Ma age for the alkalic basalts at Site 801 offers an important tie point in the calibration of the GTS. The alkalic basalts are overlain by radiolarian-bearing sediments indicative of the middle *Tricolocapsa conexa* zone, which correlates to the Bathonian-Callovian boundary or upper half of the Bathonian (Matsuoka, this volume, chapter 10). The 157.4 Ma age is younger than the 161.3 Ma value suggested for this boundary by Harland et al. (1990), but is within the uncertainty of 3 to 5 m.y. suggested by them for that part of the GTS. However, this age is significantly younger than the 169 Ma age suggested by Kent and Gradstein (1985), and suggests that the refinements in the GTS made by Harland et al. (1990) are a significant improvement, at least for the Late Jurassic. Because of ambiguities in the correlation of the Pacific Jurassic radiolarian zones with the European stages, and because of the lack of magnetic anomalies older than M37, a more precise tie of this radiometric age with the GTS may not be possible yet. The limiting constraint for this part of the time scale now seems to be the resolution of the biostratigraphy rather than the accuracy of the radiometric ages.

Pessagno and Blome (1990) report a 154 ± 1.5 Ma age for the Oxfordian-Kimmeridgian boundary, not significantly different from the 154.7 Ma reported by Harland et al. (1990), but about 5 m.y. older than one extrapolated from our age for the latest Bathonian. However, B. Murchey (pers. comm., 1991) concludes that the diagnostic Subzone 2 Gamma of Passagno and Blome (1990), defined as between the first occurrence of *Mirifusus* and the last occurrence of *Xiphostylus*, is correlative with the *Tricolopasa plicarum* and *Tricolapsa conexa* zones of Matsuoka and Yao (1986). Matsuoka (this volume) correlates these zones with the A0 and A1 zones of Baumgartner (1984, 1987), assigned to the Bajocian through Callovian stages rather than the Oxfordian assignment of Pessagno and Blome (1990). Also, the 157 ± 1.5 Ma U/Pb age of Saleeby (1987) from the Rogue Formation of Oregon (U.S.A.) is consistent with this result when the zonations of Baumgartner (1984, 1987), Matsuoka and Yao (1986), and Matsuoka (this volume) are used rather than those of Pessagno and Blome (1990).

The 157.4 Ma age for the alkalic basalt is 5 to 10 m.y. younger than that predicted by extrapolation of the M-sequence anomalies (Fig. 2). It is 10 m.y. younger than the 166.8 Ma age of the tholeiites, and the two ages are significantly different at the 95% confidence level. However, the age for the alkalic basalts is consistent with Bathonian-Callovian radiolarian age of the overlying sediments, which is also younger than the extrapolated crustal age (Fig. 2). The major and trace element geochemistry of the alkalic basalts indicates a significant contribution from an ocean island basalt (OIB) source (Floyd et al., 1991; Floyd and Castillo, this volume). The isotopic geochemistry also indicates a significant contribution from an ocean island basalt source, and Castillo et al. (this volume) suggest that the alkalic basalts are products of a mixture of the depleted mantle source of the Site 801 tholeiites and the OIB mantle source of the Site 800 alkalic dolerites. However, it is important to note that the location of the melting anomaly that created the Jurassic-age alkalic basalts at Site 801, although still within the SOPITA, is significantly removed from the location of the source of the Cretaceous-age HIMU basalts of the Pigafetta Basin and Marshall Islands (Fig. 7).

The difference in age between the 801 tholeiitic and alkalic basalts, the presence of the hydrothermal deposit separating the two sequences, and the geochemistry of the alkalic basalts all suggest that the alkalic basalts were erupted in an off-ridge environment. However, the Site 801 alkalic basalts are only about 60 m thick, and the bathymetric and seismic data around Site 801 suggests a relatively flat, normal seafloor (Lancelot, Larson, et al., 1990). This suggests that the upper sequence alkalic basalts may be more related to isolated,

Table 5. Incremental heating and laser fusion data for whole-rock samples from Hole 802A (East Mariana Basin).

Step	$^{40}Ar/^{39}Ar^a$	$^{37}Ar/^{39}Ar^a$	$^{36}Ar/^{39}Ar^a$	$^{40}Ar_R{}^b$	$^{40}Ar_K{}^b$	$^{39}Ar_{Ca}{}^b$	$^{36}Ar_{Ca}{}^b$	K/Ca	^{39}Ar (%)	Apparent age[c] (Ma)
802A-62R-2, 45–50 cm			Basalt core		$J = 0.005181$				Total gas age =	122.01 ± 1.57
[d]600	34.83	13.247	0.07116	42.6	0.0	0.9	5.0	0.037	8.5	134.84 ± 6.91
700	22.82	18.013	0.03158	65.3	0.0	1.2	15.3	0.027	13.1	135.84 ± 4.47
800	18.793	36.78	0.02863	70.5	0.0	2.5	34.6	0.0130	18.9	122.69 ± 3.14
900	15.192	37.34	0.017771	84.9	0.1	2.5	56.5	0.0128	19.2	119.61 ± 3.08
1050	14.047	20.88	0.009893	90.9	0.1	1.4	56.8	0.023	21.4	117.20 ± 2.76
1300	16.641	111.90	0.04705	69.9	0.1	7.5	64.0	0.0041	18.9	113.80 ± 3.25
802A-62R-2, 45–50 cm			Basalt core		$J = 0.004995$				Total gas age =	115.32 ± 2.93
[d]600	34.19	13.780	0.07519	38.2	0.0	0.9	4.9	0.035	8.0	115.03 ± 14.73
700	22.76	16.714	0.03355	62.2	0.0	1.1	13.4	0.029	12.0	124.67 ± 9.68
800	19.450	32.77	0.02944	68.6	0.0	2.2	29.9	0.0146	17.4	118.95 ± 6.70
900	15.524	37.22	0.019394	82.1	0.1	2.5	51.6	0.0128	18.8	114.07 ± 6.24
1050	14.540	19.875	0.011496	87.4	0.1	1.3	46.5	0.024	23.0	112.52 ± 5.08
1400	18.044	130.82	0.05694	64.3	0.1	8.8	61.8	0.0034	20.7	111.15 ± 5.74
802A-62R-3, 4–12 cm			Basalt core		$J = 0.01107$				Total gas age =	118.88 ± 2.65
[d]600	20.20	10.153	0.04614	36.4	0.0	0.7	5.9	0.048	9.5	142.26 ± 11.72
700	12.202	14.484	0.02333	52.9	0.1	1.0	16.7	0.034	11.2	125.68 ± 10.01
800	12.559	35.88	0.03265	45.8	0.1	2.4	29.6	0.0133	22.9	114.11 ± 5.00
Fuse	10.028	88.85	0.03881	56.0	0.1	6.0	61.6	0.0052	56.5	115.51 ± 3.01

[a]Corrected for ^{37}Ar and ^{39}Ar decay, half-lives are 35.1 days and 259 years, respectively.
[b]Subscripts indicate radiogenic (R), calcium-derived (Ca), and potassium-derived (K) argon.
[c]Lambda E = 0.581E-10/yr, Lambda B = 4.692E-10/yr. Errors are standard deviation of analytical precision.
[d]Temperature of each incremental heating step (°C) using a resistance furnace for heating.

relatively small alkalic seamounts formed near mid-ocean ridges rather than to a large intraplate seamount or island chain (Castillo et al., this volume; Castillo and Batiza, 1989; Zindler et al., 1984).

Site 802

The age of the Site 802 basalts is indistinguishable from the 110.8 ± 1.0 Ma age of two basalt flows from the bottom of Site 462A in the Nauru Basin (Pringle, 1992). Geochemically, the two provinces are similar, with major and trace element compositions showing a MORB affinity, while the isotopic compositions indicate some contribution from an ocean island basalt source (Castillo et al., this volume; Floyd et al., this volume; Castillo et al., 1991). The isotopic compositions of the basalts recovered from these basins (Castillo et al., 1991; Castillo et al., this volume) are significantly different than those reported for the Cretaceous SOPITA (Staudigel et al., 1991) but are similar to those found for the Ontong Java Plateau (Mahoney and Spencer, 1991; Mahoney et al., in press). I suggest that both the Nauru and East Mariana Basins are the result of rifting and extension related to the formation of Ontong Java plateau ca. 120 Ma, perhaps analogous to the dynamic relationship between the North Hawaiian Arch Flow and the Hawaiian hotspot (Clague et al., 1990).

It is important to note that the backtracked locations of the melting anomalies which formed both Ontong Java Plateau and the East Mariana and Nauru Basin basalts are significantly south of the modern SOPITA (open symbols, Fig. 7). Also, the Louisville Ridge hotspot, which has been attributed to the Ontong Java Plateau when backtracked to around 120 Ma, has been consistently decreasing in eruption rate for at least 40 Ma and appears to have no recent island or seamount volcanism associated with it. This may indicate that both the geographic extent and ocean crust production rate of the SOPITA was much greater during the Cretaceous than today (for example, Larson, 1991), and that the mantle source compositions of the Cretaceous SOPITA were more diverse than suggested by Staudigel et al. (1991). However, I prefer the alternative interpretation that the Ontong Java Plateau, East Mariana Basin, and Nauru Basin basalt provinces did not have the same origin in the SOPITA as other Cretaceous seamount provinces found in the western Pacific today.

ACKNOWLEDGMENTS

This study would not have been possible without Pat Castillo's help with initial sample selection at sea, Roger Larson's answering and fax machines, and Hubert Staudigel's advice to always avoid overcommitting oneself while convincing me to overcommit myself and accept an invitation to join the Leg 129 scientific staff. Debbie Christianson provided timely mineral separations from limited material. Mike McWilliams and Phil Gans provided ready access to their new argon facility at Stanford. Walter H.F. Smith patiently instructed the author in the use of the GMT plotting software (Wessel and Smith, 1991). G. Brent Dalrymple, Bill Sliter, Roger Larson, Tracey Vallier, and John O'Conner provided helpful reviews of the manuscript.

REFERENCES

Baumgartner, P. O., 1984. A Middle Jurassic-Early Cretaceous low-latitude radiolarian zonation based on Unitary Associations and age of Tethyan radiolarites. *Eclogae Geol. Helv.*, 77:729–837.

———, 1987. Age and genesis of Tethyan Jurassic radiolarites. *Eclogae Geol. Helv.*, 80:831–879.

Brooks, C., Hart, S. R., and Wendt, I., 1972. Realistic use of two-error regression treatments as applied to rubidium-strontium data. *Rev. Geophys. Space Phys.*, 10:551–557.

Castillo, P. R., and Batiza, R., 1989. Sr, Nd, and Pb isotope constraints on near-ridge seamount production beneath the South Atlantic. *Nature*, 342:262–265.

Castillo, P. R., Carlson, R. W., and Batiza, R., 1991. Origin of Nauru Basin igneous complex: Sr, Nd, and Pb isotope and REE constraints. *Earth Planet. Sci. Lett.*, 103:200–213.

Clague, D. A., Dalrymple, G. B., and Moberly, R., 1975. Petrography and K-Ar ages of dredged volcanic rocks from the western Hawaiian ridge and southern Emperor seamount chain. *Geol. Soc. Am. Bull.*, 84:991–998.

Clague, D. A., Holcomb, R. T., Sinton, J. M., Detrick, R. S., and Torresan, M. E., 1990. Pliocene and Pleistocene alkalic flood basalts on the seafloor north of the Hawaiian islands. *Earth Planet. Sci. Lett.*, 98:175–191.

Dalrymple, G. B., 1989. The GLM continuous laser system for $^{40}Ar/^{39}Ar$ dating: description and performance characteristics. *U.S. Geol. Surv. Bull.,* 1890:89–96.

Dalrymple, G. B., Alexander, E. C., Lanphere, M. A., and Kraker, G. P., 1981. Irradiation of samples for $^{40}Ar/^{39}Ar$ dating using the Geological Survey TRIGA reactor. *Geol. Surv. Prof. Pap. U.S.,* 1176:1–55.

Dalrymple, G. B., and Clague, D. A., 1976. Age of the Hawaiian-Emperor Bend. *Earth Planet. Sci. Lett.,* 31:313–329.

Dalrymple, G. B., and Duffield, W. A., 1988. High precision $^{40}Ar/^{39}Ar$ dating of Oligocene rhyolites from the Mogollon-Datil Volcanic Field using a continuous laser system. *Geophys. Res. Lett.,* 14:462–464.

Dalrymple, G. B., Lanphere, M. A., and Clague, D. A., 1980. Conventional and $^{40}Ar/^{39}Ar$ ages of volcanic rocks from Ojin (Site 430), Nintoku (Site 432), and Suiko (Site 433) Seamounts, and the chronology of volcanic propogation along the Hawaiian-Emperor chain. *In* Jackson, E. D., Koizumi, I., et al., *Init. Repts. DSDP,* 55: Washington (U.S. Govt. Printing Office), 659–676.

Dalrymple, G. B., Lanphere, M. A., and Pringle, M. S., 1988. Correlation diagrams in $^{40}Ar/^{39}Ar$ dating: is there a correct choice? *Geophys. Res. Lett.,* 15:589–591.

Davis, A. S., Pringle, M. S., Pickthorn, L.B.G., Clague, D. A., and Schwab, W. C., 1989. Petrology and age of alkalic lava from the Ratak chain of the Marshall Islands. *J. Geophys. Res.,* 94:9757–9774.

Duncan, R. A., and Clague, D. A., 1985. Pacific plate motions recorded by linear volcanic chains. *In* Nairn, A.E.M., Stehli, F. G., and Uyeda, S. (Eds.), *The Ocean Basins and Margins* (Vol. 7A): New York (Plenum), 89–91.

Fleck, R. J., Sutter, J. F., and Elliot, D. H., 1977. Interpretation of discordant $^{40}Ar/^{39}Ar$ age spectra of Mesozoic tholeiites from Antartica. *Geochim. Cosmochim. Acta,* 41:15–32.

Floyd, P. A., Castillo, P. R., and Pringle, M. S., 1991. Tholeiitic and alkalic basalts of the oldest Pacific Ocean crust. *Terra Nova,* 3:257–265.

Gradstein, F. M., and Sheridan, R. E., 1983. On the Jurassic Atlantic Ocean and a synthesis of results of DSDP Leg 76. *In* Sheridan, R. E., Gradstein, F. M., et al., *Init. Repts. DSDP,* 76: Washington (U.S. Govt. Printing Office), 913–943.

Handschumacher, D. M., and Gettrust, J. F., 1985. Mixed polarity model for the Jurassic "Quiet Zones": new oceanic evidence of frequent pre-M25 reversals. *Eos,* 66:867.

Handschumacher, D. M., Sager, W. W., Hilde, T.W.C., and Bracey, D. R., 1988. Pre-Cretaceous tectonic evolution of the Pacific plate and the extension of the geomagnetic time scale with implications for the origin of the Jurassic "Quiet Zone." *Tectonophysics,* 155:365–380.

Harland, W. B., Armstrong, R. L., Cox, A. V., Craig, L. E., Smith, A. G., and Smith, D. G., 1990. *A Geologic Time Scale:* Cambridge (Cambridge Univ. Press).

Kent, D. V., and Gradstein, F. M., 1985. A Cretaceous and Jurassic geochronology. *Geol. Soc. Am. Bull.,* 96:1410–1427.

Lancelot, Y., Larson, R. L., et al., 1990. *Proc. ODP, Init. Repts.,* 129: College Station, TX (Ocean Drilling Program).

Lanphere, M. A., and Dalrymple, G. B., 1978. The use of $^{40}Ar/^{39}Ar$ data in the evaluation of disturbed K-Ar systems. *In* Zartman, R. E. (Ed.), *Short Papers on the Fourth International Conference on Geochronology, Cosmochronology, and Isotope Geology.* Open-File Rep.—U.S. Geol. Surv., 78-701:241–243.

Larson, R. L., 1991. Latest pulse of the earth: evidence for a mid-Cretaceous superplume. *Geology,* 19:547–550.

Larson, R. L., and Hilde, T.W.C., 1975. A revised time scale of magnetic reversals for the Early Cretaceous and Late Jurassic. *J. Geophys. Res.,* 80:2586–2594.

Mahoney, J. J., and Spencer, K. J., 1991. Isotopic evidence for the origin of the Manihiki and Ontong Java plateaus. *Earth Planet. Sci. Lett.,* 104:196–210.

Mahoney, J. J., Storey, M., Duncan, R. A., Spencer, K. J., and Pringle, M. S., in press. Geochemistry and geochronology of the Ontong Java Plateau. *In* Pringle, M. S., Sager, W. W., Sliter, W., and Stein, S. (Eds.), *The Mesozoic Pacific (Schlanger Volume).* Am. Geophys. Union, Geophys. Monogr. Ser.

Mankinen, E. A., and Dalrymple, G. B., 1972. Electron microprobe evaluation for whole rock K-Ar dating. *Earth Planet. Sci. Lett.,* 17:89–94.

Matsuoka, A., and Yao, A., 1986. A newly proposed radiolarian zonation for the Jurassic of Japan. *Mar. Micropaleontol.,* 11:91–106.

McIntyre, G. A., Brooks, C., Compston, W., and Turek, A., 1966. The statistical assessment of Rb-Sr isochrons. *J. Geophys. Res.,* 71:5459–5468.

Ozima, M., Honda, M., and Saito, K., 1977. $^{40}Ar/^{39}Ar$ ages of guyots in the western Pacific and discussion of their evolution. *Geophys. J. R. Astron. Soc.,* 51:475–485.

Pessagno, E. A., and Blome, C. D., 1990. Implications of new Jurassic stratigraphic, geochronometric, and paleolatitude data from the western Klamath terrane (Smith River and Rogue River subterranes). *Geology,* 18:665–668.

Pringle, M. S., 1992. Geochronology and petrology of the Musician Seamounts, and the search for hotspot volcanism in the Cretaceous Pacific [Ph.D. dissert.]. Univ. of Hawaii at Manoa, Honolulu.

Saleeby, J. B., 1987. Discordance patterns in Pb/U zircon ages of the Sierra Nevada and Klamath Mountains. *Eos,* 68:1514–1515.

Schlanger, S. O., Gracia, M. O., Keating, B. H., Naughton, J. J., Sager, W. W., Haggerty, J. A., Philpotts, J. A., and Duncan, R. A., 1984. Geology and geochronology of the Line Islands. *J. Geophys. Res.,* 89:11201–11272.

Siedemann, D. A., 1978. $^{40}Ar/^{39}Ar$ studies of deep-sea igneous rocks. *Geochim. Cosmochim. Acta,* 42:1721–1724.

Smith, W.H.F., Staudigel, H., Watts, A. B., and Pringle, M. S., 1989. The Magellan Seamounts: Early Cretaceous record of the South Pacific isotopic and thermal anomaly. *J. Geophys. Res.,* 94:10501–10523.

Staudigel, H., Park, K.-H., Pringle, M. S., Rubenstone, J. L., Smith, W.H.F., and Zindler, A., 1991. The longevity of the south Pacific isotopic and thermal anomaly. *Earth Planet. Sci. Lett.,* 102:24–44.

Tamaki, K., Nakanishi, M., Sayanagi, K., Kobayashi, K., 1987. Jurassic magnetic anomaly lineations of the western Pacific Ocean and the origin of the Pacific plate. *Eos,* 68:1493.

Taylor, J. R., 1982. *An Introduction to Error Analysis:* Mill Valley, CA (Univ. Science Books).

Turner, D. L., and Jarrard, R. D., 1982. K-Ar dating of the Cook-Austral island chain: a test of the hotspot hypothesis. *J. Volcanol. Geotherm. Res.,* 12:187–220.

Watts, A. B., Weissel, J. K., Duncan, R. A., and Larson, R. L., 1987. Origin of the Louisville ridge and its relationship to the Eltanin fracture zone. *J. Geophys. Res.,* 93:3051–3077.

Wessel, P., and Smith, W.H.F., 1991. GMT: a public domain UNIX software package for data manipulation and presentation using the PostScript page description language. *Eos,* 72:441.

York, D., 1969. Least squares fitting of a straight line with correlated errors. *Earth Planet. Sci. Lett.,* 5:320–324.

Zindler, A., Staudigel, H., and Batiza, R., 1984. Isotope and trace element geochemistry of young Pacific seamounts: implications for the scale of upper mantle heterogeneity. *Earth Planet. Sci. Lett.,* 70:175–195.

Zotto, M., Drugg, W. W., and Habib, D., 1987. Kimmeridgian dinoflagellate stratigraphy in the Southwestern North Atlantic. *Micropaleontology,* 33:193–213.

Date of initial receipt: 4 November 1991
Date of acceptance: 31 March 1992
Ms 129B-130

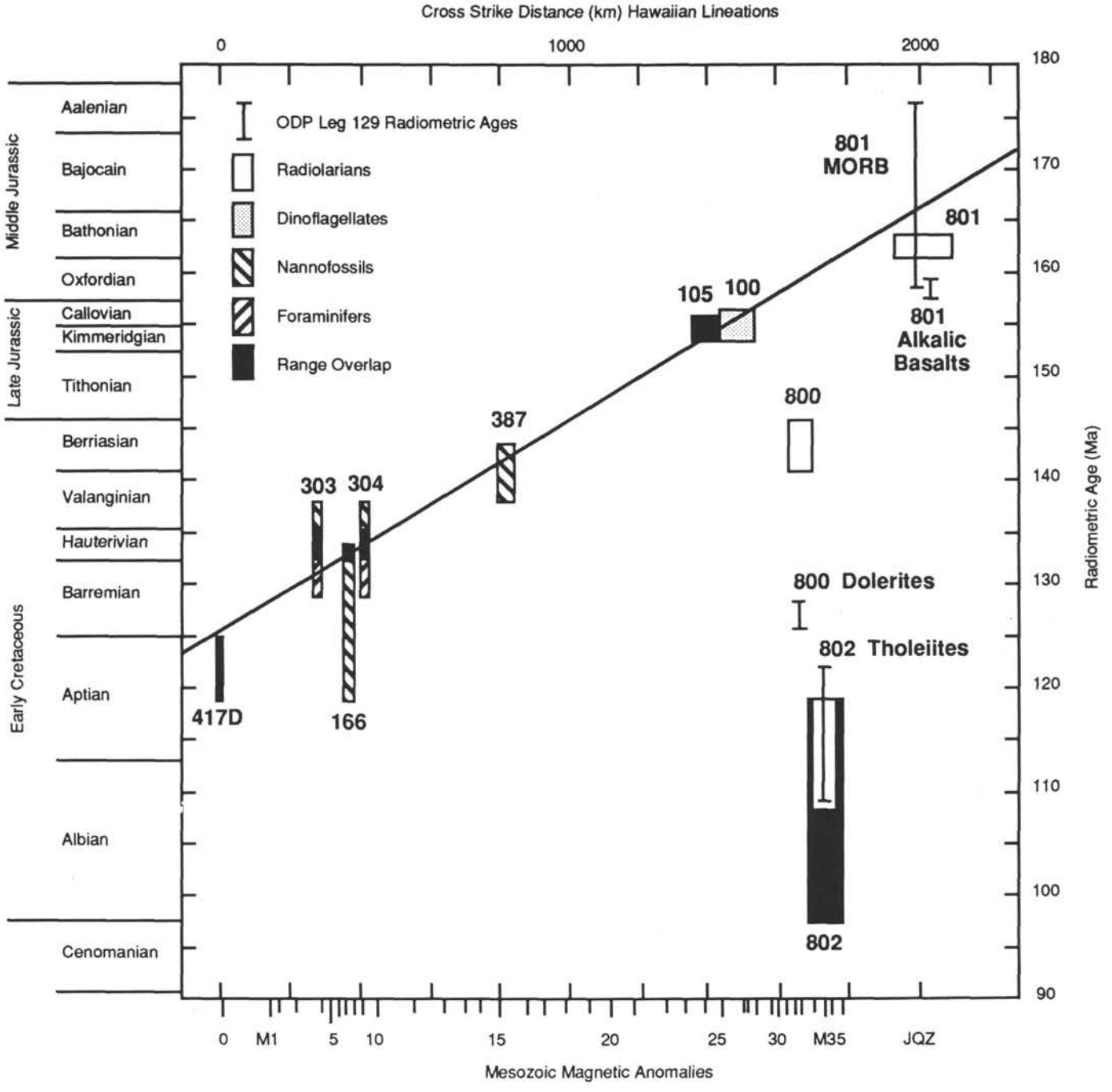

Figure 2. Time calibration plot of the Mesozoic anomalies M0 to M37 and the preceding Jurassic magnetic quiet zone (JQZ). Modified from Lancelot, Larson, et al. (1990) using the time scale of Harland et al. (1990). Magnetic anomalies are plotted as cross-strike distance across the Hawaiian lineations for M0 to M25. Anomalies M25 to M37 are normalized to that pattern after Handschumacher et al. (1988). Ages of various DSDP holes (numbered) are shown in rectangles. Vertical lengths of rectangles show paleontologic age ranges from DSDP intial reports, except for 100 (Zotto et al., 1987) and 105 (Gradstein and Sheridan, 1983). Horizontal lengths show magnetic ages ranges from Larson and Hilde (1975) for Sites 303, 304, 166, 100, and 105, from DSDP Initial Reports for Site 387 and Hole 417D, and ODP Leg 129 Vol. A for Sites 800, 801, and 802. Radiometric ages from Sites 800, 801, and 802 are shown as ties lines, ±2 s.d. long.

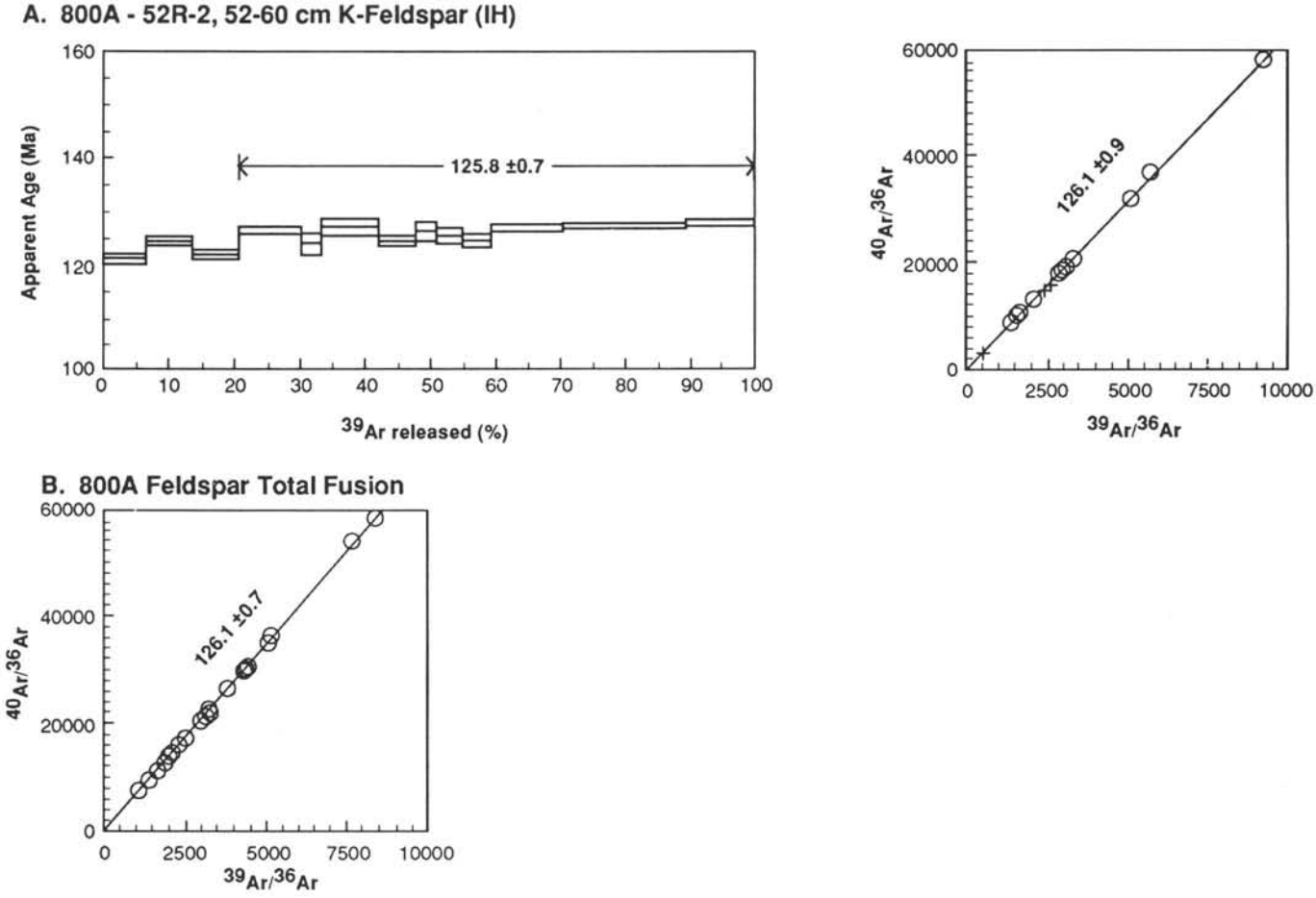

Figure 3. $^{40}Ar/^{39}Ar$ laser analyses of feldspar separates from Hole 800A, Leg 129. **A.** Age spectra and isochron for a laser incremental-heating experiment. **B.** Laser-fusion isochron for feldspar separates from both 52R-2, 52–60 cm and 61R-1, 17–24 cm.

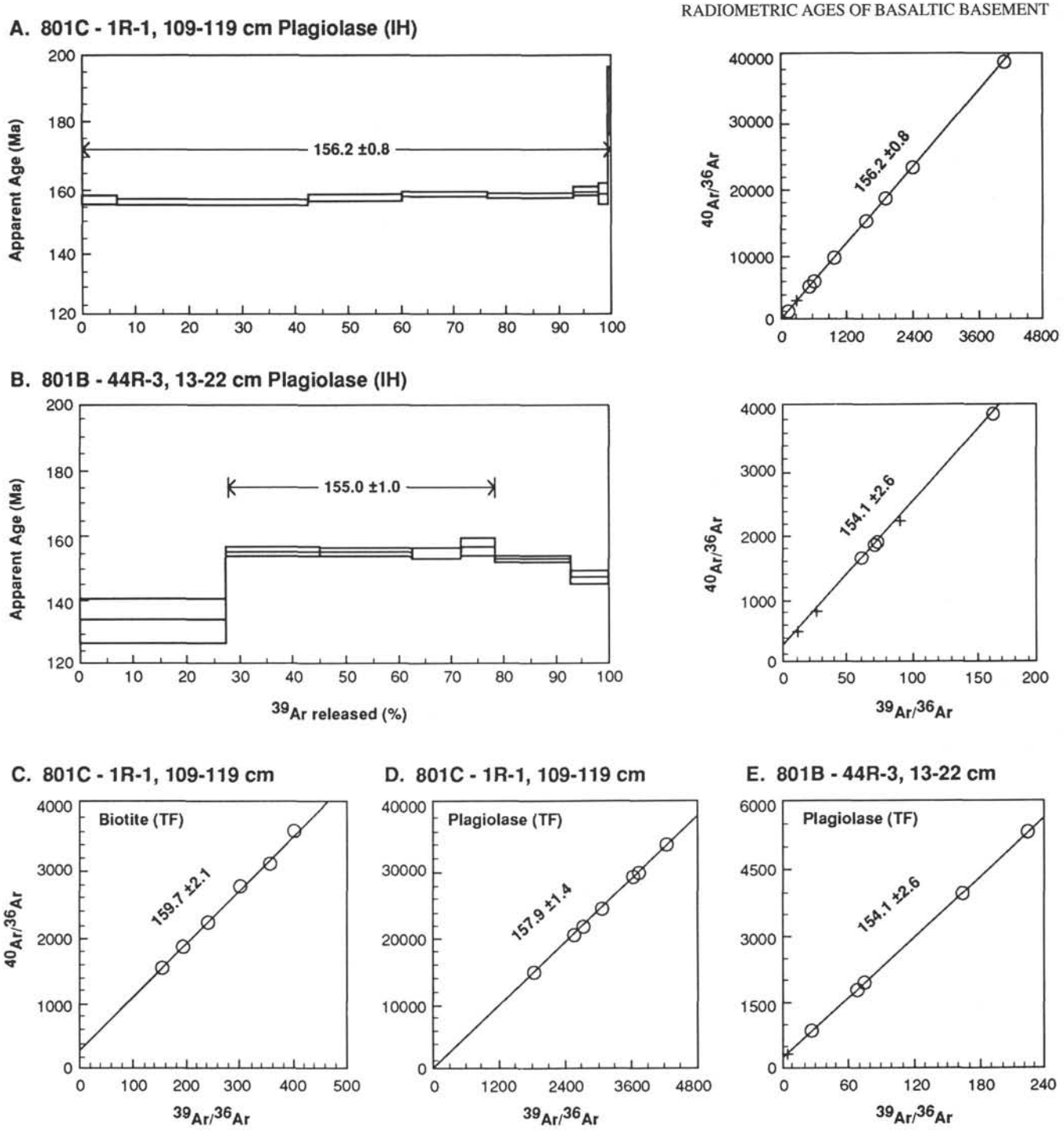

Figure 4. $^{40}Ar/^{39}Ar$ laser fusion and resistance furnace incremental-heating experiments for plagioclase and biotite separates from the alkalic basalts recovered at Holes 801B and 801C, Leg 129. **A.** Resistance furnace incremental-heating age spectrum and isochron. **B.** Resistance furnace incremental-heating age spectrum and isochron. **C.** Laser-fusion isochron. **D.** Laser-fusion isochron. **E.** Laser-fusion isochron.

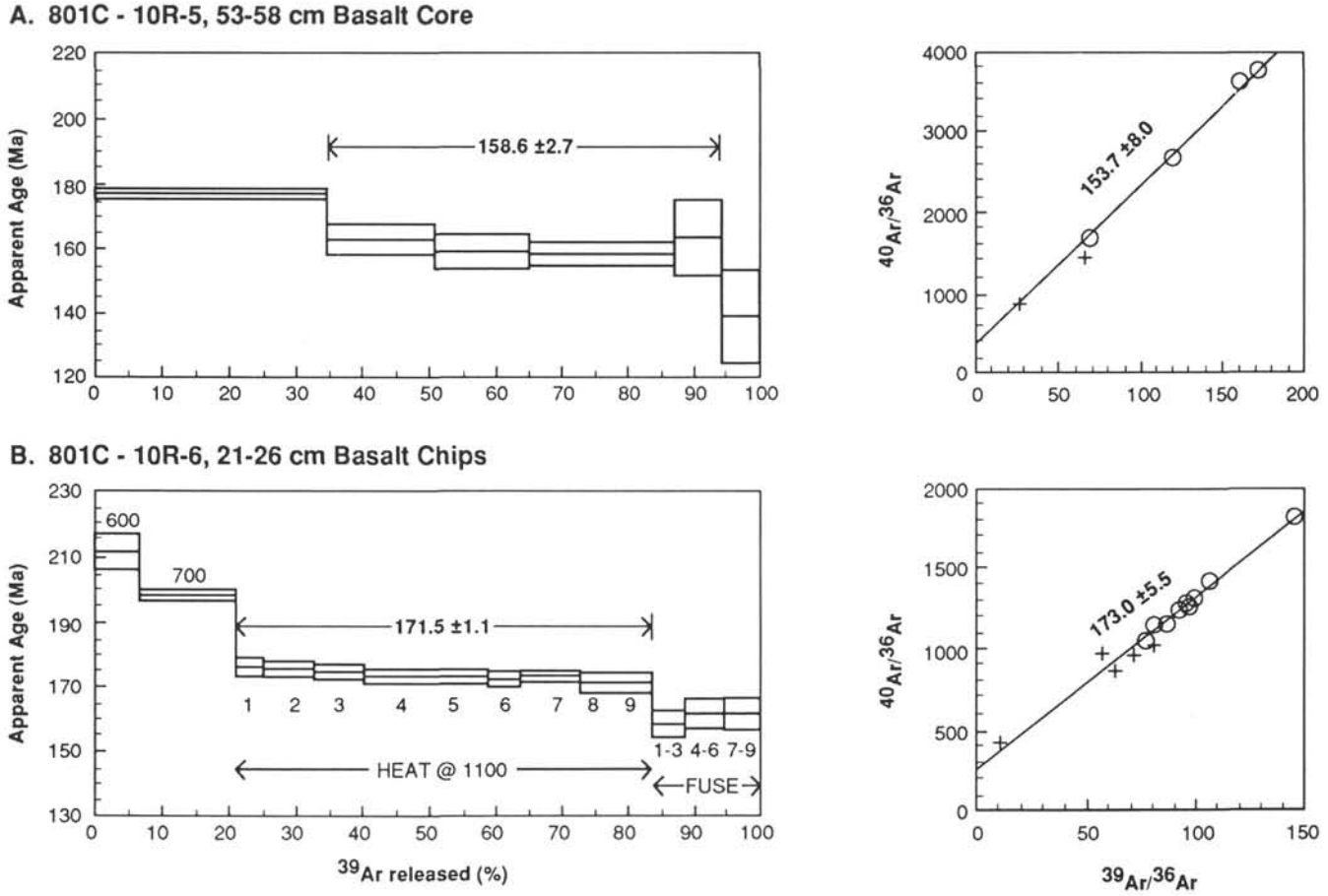

Figure 5. $^{40}Ar/^{39}Ar$ resistance furnace and laser-heating of samples from the tholeiitic basalts of Hole 801C, Leg 129. **A.** Resistance furnace incremental-heating age spectrum and isochron. **B.** Laser-heating of nine individual basalt chips weighing 2–4 mg each. Chips were first degassed together in two steps at 600°C and 700°C, then heated at 1100°C and measured individually, and finally fused in three groups of three each.

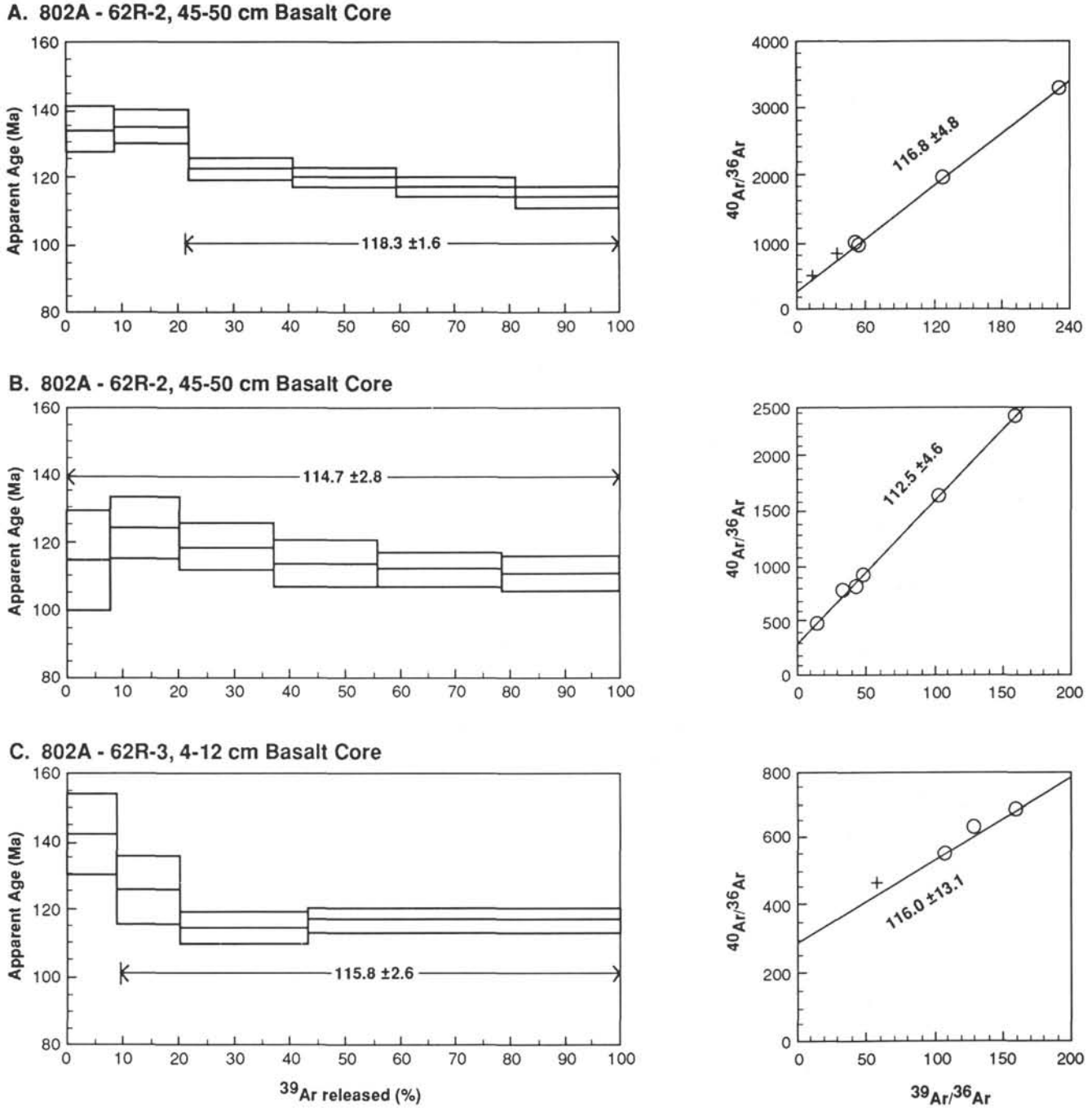

Figure 6. $^{40}Ar/^{39}Ar$ whole rock incremental-heating experiments on three samples from Hole 802A, Leg 129. Age spectra are shown on the left, isochrons on the right.

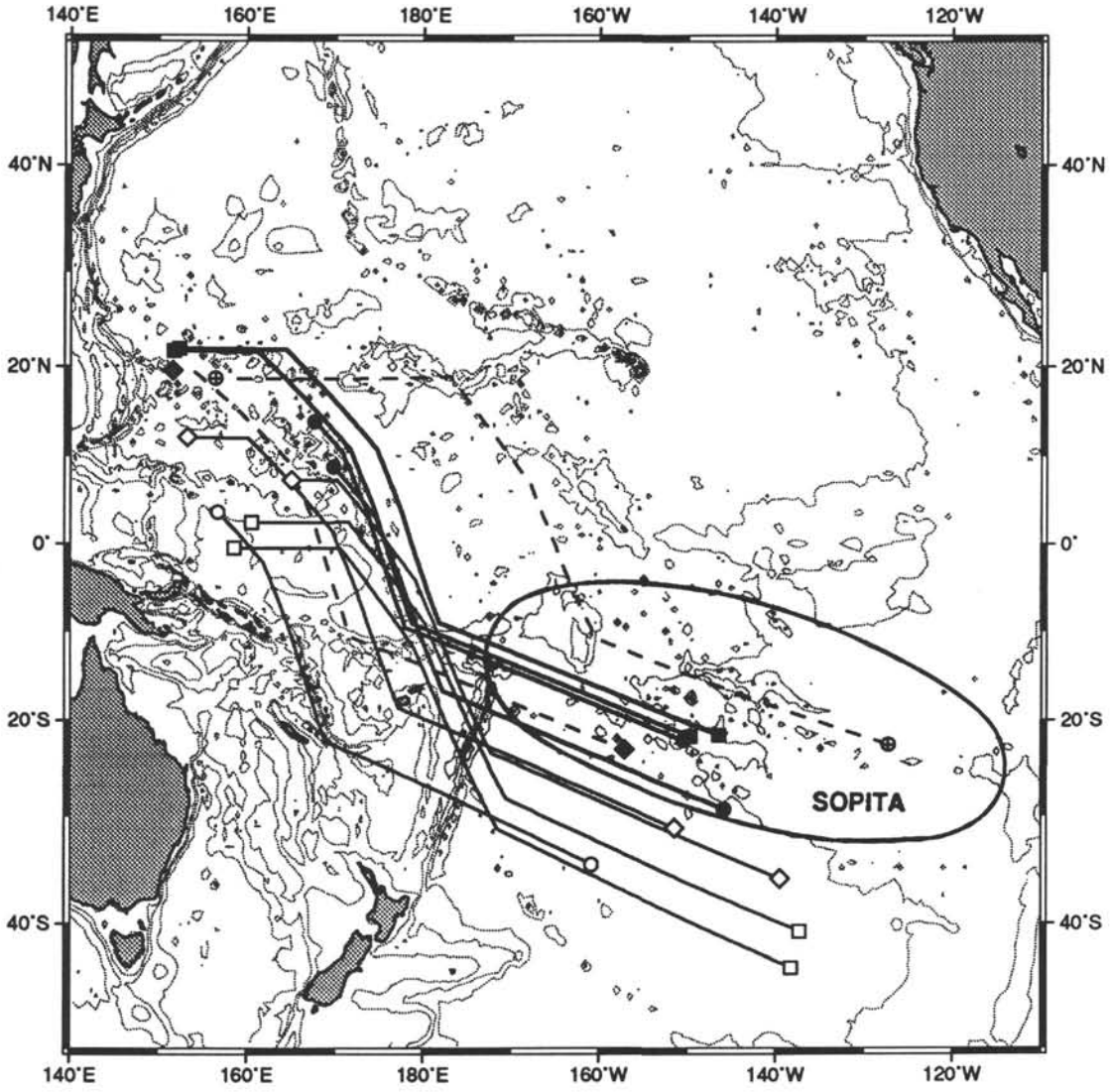

Figure 7. Locations of the melting anomalies which formed the eleven sites of Mesozoic volcanism shown in Figure 1, and model hotspot traces left on the Pacific plate as the plate moved over each of the locations since those sites were formed. Model hotspot traces calculated using the rotation poles of Duncan and Clague (1985) and ages from this study for Sites 800, 801, and 802; from Mahoney et al. (in press) for Sites 289, 803, and 807; from Pringle (1992) for Himu, Hemler, and Hole 462A; and from Davis et al. (1989) for Erikub and Ratak. Figure drawn using the GMT mapping utilities of Wessel and Smith (1991).